Frequency Adjustable Dual-Band Microstrip Gap-Ring-Slot Antenna Design Using the Cylindrical TLM Method

Tijana Z. Dimitrijevic, Jugoslav J. Jokovic, and Nebojsa S. Doncov

Faculty of Electronic Engineering
University of Niš, Niš, 18000, Serbia
tijana.dimitrijevic@elfak.ni.ac.rs, jugoslav.jokovic@elfak.ni.ac.rs, nebojsa.doncov@elfak.ni.ac.rs

Abstract ─ This paper introduces a design of a frequency adjustable dual-band circular patch antenna with a gap-ring-slot accompanied by a study of a cylindrical TLM method effectiveness and capabilities. The antenna is fabricated on Rogers 4003 substrate and measured results have been used to validate the used approach. Through comparison with corresponding rectangular TLM mesh results, the cylindrical TLM method has been found not only as more efficient requesting much smaller number of cells to be applied but also more capable to accurately describe narrow ring slots and small angular features. The designed antenna resonates at two frequencies, 2.77 GHz and 3.72 GHz, with the possibility of additional frequency tuning. A frequency adjustments study has been carried out and, accordingly, design corrections have been proposed either to independently tune the frequency or to simultaneously adjust both frequencies.

Index Terms ─ Cylindrical meshing, dual-band patch antennas, frequency tuning, gap ring slot, transmission line-matrix method.

I. INTRODUCTION

Nowadays rapid development of wireless communication systems puts a high demand on the design of devices for various services requesting miniaturized multipurpose antennas to be used that are preferably to support multi-frequency operation with desired radiation characteristics. Accordingly, practising the most versatile, the most feasible and the most accurate design methodology for low-profile and compact antennas is inevitable, yielding enhancement of established numerical techniques as well as the generation of hybrid or some novel techniques in conjunction with the development of commercial or in-house solvers [1-4].

Available approximate techniques, such as the cavity model or the transmission line modelling, are applicable only in simplified cases of the microstrip patch antennas [1,2]. Therefore, a usage of a relevant full-wave method that allows modelling of a complex geometry while taking into account inhomogeneous materials, wire elements and boundaries, emerges as a good starting point in the antenna design. There are many full-wave methods that are widely used in the area of electromagnetic field propagation modelling, such as Method of Moments (MoM) [5], Finite-Difference Time-Domain (FD-TD) [6], Finite Element Method (FEM) [7], Transmission-Line Matrix (TLM) method [3] etc. No solution is perfectly accurate and it is the designer's decision to choose which one is to be used while fulfilling specific requirements in terms of the geometry or purpose.

Among various designs of microstrip patch antennas, annular-ring patch antennas and annular-slot antennas have attracted a significant interest because of their appealing features such as a miniaturized configuration, light weight, ease of fabrication and compatibility with small portable units for wireless communication. A circular patch-ring antenna with a wide bandwidth, designed by TLM, was presented in [8]. A multi-frequency operation of microstrip-fed slot-ring antennas on thin substrates with a low-dielectric permittivity was investigated using the Integral Equation MoM simulator [9]. FEM was used to design strip-loaded annular-ring microstrip patch antennas [10], while an asymmetric feedline was used to excite multiple modes on an annular-ring slot antenna in [11]. A dual-band annular slot antenna for radio base stations and bidirectional radiated circularly polarized annular-ring slot antenna for a portable RFID reader were also designed using FEM [12,13].

In addition to antenna compactness, multi-functionality plays an important role in modern wireless communications as well. Hence, design of multiband antennas and frequency reconfigurable antennas has gained a full attention among researchers. As inferred from published literature, different techniques have been applied to achieve a multiband operation for antennas. By embedding narrow open rectangular ring slot close to the boundary of a rectangular patch of single layer and single feed, dual frequency operation was obtained in antenna designed using FEM in [14]. By using inverted-L- and T-shaped parasitic elements a multiband antenna

Submitted On: October 5, 2018
Accepted On: December 27, 2018

1054-4887 © ACES

was developed [15], whereas a substrate-integrated waveguide (SIW) cavity-backed annular ring slot antenna was designed by FEM in [16].

Notwithstanding their flexibility and efficiency, the numerical computational methods face many problems and limitations when modelling of structures containing curvilinear surfaces is concerned. Therefore, conformity of the mesh is an important issue that has to be pointed out in a microstrip antenna design since it affects the modelling solution in two manners: one is a demand to accurately describe curvilinear boundaries and material surfaces, and the other is consumption of available computational resources in the most effective way, both in terms of simulation time and memory. The TLM method [3] is a well-established method and used by commercial software packages, such as the CST Microwave Studio [4], enabling modelling and analyses of complex microwave structures and devices. It is originally developed in the rectangular coordinate system with a basic cubic cell [3]. Although it is proved to be efficient in versatile cases, there are cases, however, where usage of staircase approximation for describing curvilinear surfaces leads to increased simulation run-time, greater memory requirements and sometimes numerical errors [17, 18]. Recently developed UTLM (Unstructured TLM), based on unstructured meshes (triangular, tetrahedral) provides better conformity of the mesh, but it may also be computationally more demanding [19, 20]. Therefore, the authors of this paper are of the opinion that some specific structures can be more conveniently and more efficiently described using the mesh in the corresponding grid, such as, for instance, the orthogonal polar mesh applied to the circular patch antenna, [21]. A development of an in-house solver that uses the TLM method in the orthogonal polar mesh (3DTLMcyl_cw) with efficiently embedded wire model was presented in [22]. Even though its possibilities are limited to structures containing cylindrical/circular surfaces, in these cases, however, results can be reached in the most efficient manner. This advantage is especially emphasized in specific cases where narrow slots are to be described, because of the perfect adjustments of the mesh to the considered structure as explored in [8,18].

This paper is focused on the coaxially fed slotted circular patch antenna, designed using the cylindrical TLM solver, where the dual-band operation is accomplished by loading a ring slot with a small gap. Similar approach has already been used in [14], but on an example of a rectangular patch antenna. An open rectangular slot embedded near the rectangular patch boundary provides reactive loading around the resonance frequency. As a consequence, a dual frequency operation can be obtained. The proposed design here, in addition to the dual frequency operation, contains specific geometrical surfaces (circular/cylindrical), of which are especially interesting narrow radial and angular features, making it suitable to further explore possibilities and meshing/ modelling advantages of the applied method. As it will be shown in this paper, the cylindrical TLM approach has been used to design the circular antenna with dual-band operation while the approach itself has been investigated from the point of view of the modelling accuracy and efficiency. A novel, specific challenge in modelling of the structures considered in this paper can be contributed to the presence of the narrow ring slot and the small annular gap. What is more, the cylindrical TLM solver has been used to conduct a parametric study of the designed antenna allowing for additional frequency adjustments of the excited modes. Accordingly, design techniques have been proposed to achieve independent adjustment of the lower resonant mode in the frequency range of interest and tuning of both modes simultaneously.

The paper is organized through several sections. After the Introduction, Section II is devoted to a brief theory of the TLM method in a cylindrical coordinate system including the numerical procedure and modelling issues. The antenna design is presented in Section III, the frequency adjustments study is given in Section IV, whilst the cylindrical meshing capabilities together with the efficiency are explored in Section V. Verification of the approach through comparing the simulated and measured results are presented in Sections VI, after which the major conclusions are drawn.

II. CYLINDRICAL TLM APPROACH

The TLM method is a numerical method that is based on the physical model of a system, therefore, it is suitable for numerical modelling rather than just numerical analysis. As a differential method, the TLM is convenient for solving problems in inhomogeneous mediums, for considering of nonlinear characteristics and for solving problems in the time-domain. It is based on the network of transmission lines where voltages and currents are equivalently connected to electromagnetic field components defined by Maxwell's equations. A space of electromagnetic field propagation is described by the network of cells comprised of transmission lines interconnection. The basic cell is Symmetrical Condensed Node (SCN) [3], but to allow for a construction of a non-uniform mesh and to define different material properties as well as to speed up a simulation process, the hybrid symmetrical condensed nodes (HSCN) [23] can be used instead.

An in-house solver, 3DTLMcyl_cw, used in this paper for the antenna design and analysis, is developed in the cylindrical coordinate system and uses the HSCN adapted to the cylindrical grid [22]. The code has been enhanced by the implementation of the compact wire model adjusted to the cylindrical grid. The model uses a wire network consisted of link and stub lines to account for the increase of the capacitance and inductance of the medium caused by the wire and it is interposed over the

existing network of nodes [24]. The TLM wire node belonging to the straight wire segment running in z-direction is presented in Fig. 1 (a).

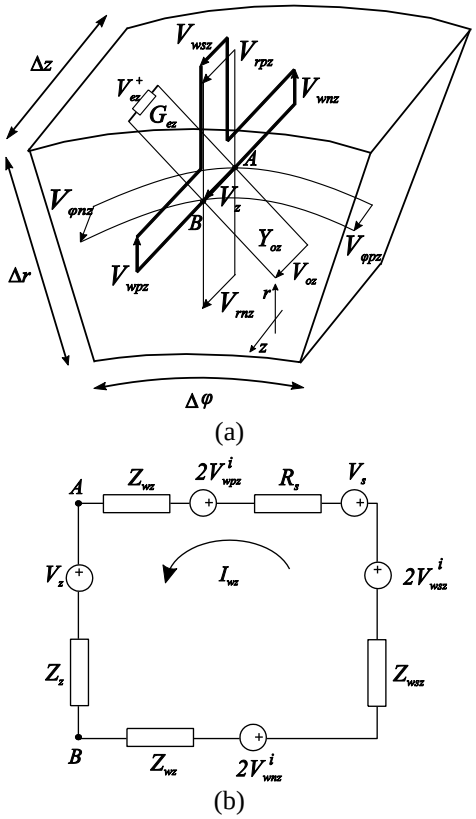

Fig. 1. (a) TLM wire node for a wire running in z-direction, and (b) Thevenin circuit for the wire segment in z-direction.

Within a scattering procedure in a wire network for a segment running in z-direction, reflected voltage pulses are calculated in specific wire nodes as follows:

$$\begin{aligned} V^r_{wnz} &= V^i_{wnz} - I_{wz} Z_{wz} \\ V^r_{wpz} &= V^i_{wpz} + I_{wz} Z_{wz} \\ V^r_{wsz} &= V^i_{wsz} - I_{wz} Z_{wsz} \end{aligned}, \tag{1}$$

and a current propagating through the wire placed along *z*-direction is determined as:

$$I_{wz} = \frac{2V^i_{wnz} + 2V^i_{wsz} - 2V^i_{wpz} - V_z - V_S}{2Z_{wz} + Z_{wsz} + Z_z + R_S}, \tag{2}$$

where V^i_{wnz}, V^i_{wpz}, and V^i_{wsz} are incident voltage pulses, V^r_{wnz}, V^r_{wpz}, and V^r_{wsz} reflected voltage pulse, V_S and R_S are the voltage and the impedance of the source connected to the wire, respectively. Z_z and V_z are calculated when regular node ports are determined using the Thevenin circuit between A and B (Fig. 1 (b)).

Boundaries in the cylindrical TLM solver can be modelled as internal or external ones, representing circular or cylindrical surfaces. An analogy between the electric field and the voltages at TLM nodes enables defining the boundaries through introducing corresponding reflection coefficients. In case of a patch antenna modeling, a perfect electric conductor (PEC) is used to describe metallic layers: a radiated patch and a ground plane. It is also possible to model conductance losses by introducing finite characteristic impedance and calculating relevant reflection coefficient which would be greater than -1. By using the reflection coefficient equal to 1, a metallic wall can be described at the center of the orthogonal polar TLM mesh with a circle of an infinitesimal circumference. Finally, the TLM network of transmission lines can be loaded with theirs characteristic impedance (i.e., ρ=0), defining an absorbing boundary, which find its purpose in modeling of open boundary structures such as the microstrip patch antennas. Namely, the boundaries of the patch antenna modeling space have to be extended beyond the realistic antenna dimensions and described as absorbing with properly calculated reflection coefficients of the link lines.

Adapting the compact wire model to the orthogonal polar mesh has enabled describing the wire elements. From the computational point of view, an implementation of the compact wire model into the cylindrical TLM algorithm resulted in additional subroutine involving calculation and exchange of link-line impedances of the nodes along which the wire passes due to different cross-section of the wire nodes. In case of patch antennas, this model can be used to model the inner coaxial wire connecting the radiated patch and the ground plane, while a voltage source of Vg=1V with an internal resistance Rg=50Ω is attached through the so-called wire port to the wire end. However, the wire element modeling faces limitation related to maximum wire radius, since it is determined by the cell size through which the wire passes. Therefore, a compromise should be made between the wire radius and the mesh resolution. Taking advantage of the conformity of the cylindrical mesh to the structures of circular/cylindrical geometry, the cylindrical mesh gives more possibilities [17], and the limitation might be overcome, especially in cases when wires are placed along radial direction, where the space discretization allows thicker wires to be embedded.

Since the TLM method demands a discretization of a modeling space, it is of importance to appropriately define a mesh resolution in order to provide a satisfactory accuracy. To provide satisfactory accuracy of results in a frequency range of interest, there is a general recommendation to use the space discretization between adjacent nodes smaller than λ/10, where λ is the wavelength and the relative permittivity is 1. In case of inhomogeneous media it is essential to ensure time

synchronism in the mesh. Therefore, the approximate wavelength is $\lambda_m = \lambda/\sqrt{\varepsilon_r}$, hence the condition $\Delta l < \lambda_m/10$ should be accomplished, where Δl represents the cell size. However, when the considered structure contains fine features, thin layers or narrow parts, the mesh of higher resolution should be applied. According to defined electromagnetic characteristics of a medium and defined space discretization, TLM algorithm calculates the time-step.

An in-house solver which is based on the TLM numerical procedure handles of all the above modeling issues. It starts with the model description through defining the problem dimensions, mesh resolution adjustments, defining media properties, setting up an impulse or a voltage source excitation and defining the wanted output result. These parameters are imported by the user within the input text file. When it runs, the solver checks imported values and handles possible errors in terms of maximum number of iterations, maximum computational area in all corresponding directions, maximum number of boundaries, metallic layers, wire elements and excitations, as well as maximum number of regions which are used to reduce computations within the same medium. After that follows imposing initial conditions and determination of link and stub lines impedances for each HSCN as well as determination of wire nodes impedances. Then, the algorithm goes through iterative stages: calculation of equivalent voltages and currents for each node (EM field components can be calculated at this stage as well), scattering procedure for regular and wire nodes, connection procedure for regular and wire nodes, modification of the connection procedure at boundaries, calculation of the current induced in the probe wire (output result) in the time domain, transforming data into the frequency domain, and calculation of S parameters or input impedance [22].

III. ANTENNA DESIGN

Design and fabrication of the dual-band coaxially fed antenna with a gap-ring-slot were preceded by the development of a model of a simple circular patch (CP) antenna of a radius 15 mm and a coaxial feed position ρ = 3.5 mm. As a substrate, Rogers 4003 with the relative permittivity ε_r = 3.38 and the height h = 1.524 mm, was used. Simulated results representing reflection coefficients for the CP antenna is shown in Fig. 2. According to the simulations in both rectangular and cylindrical TLM solvers with the same cell size along x- and y-axes, and along the r-axis (λ/60, λ corresponds to the maximum frequency of interest), the fundamental mode is excited at about 3.12 GHz.

The layout and the experimental model of the CP gap-ring-slot antenna are shown in Fig. 3.

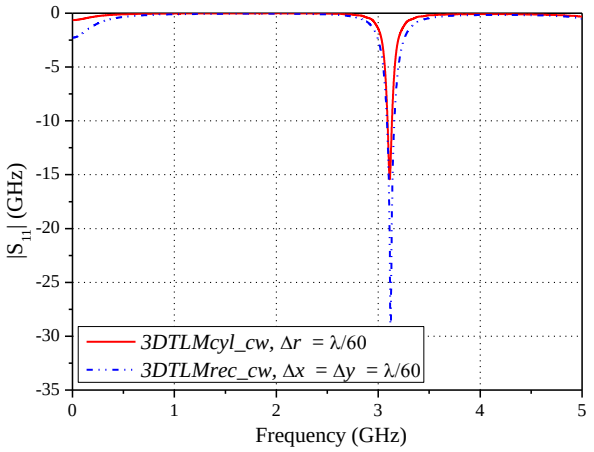

Fig. 2. Simulated reflection coefficient for the circular patch antenna of radius a = 15mm.

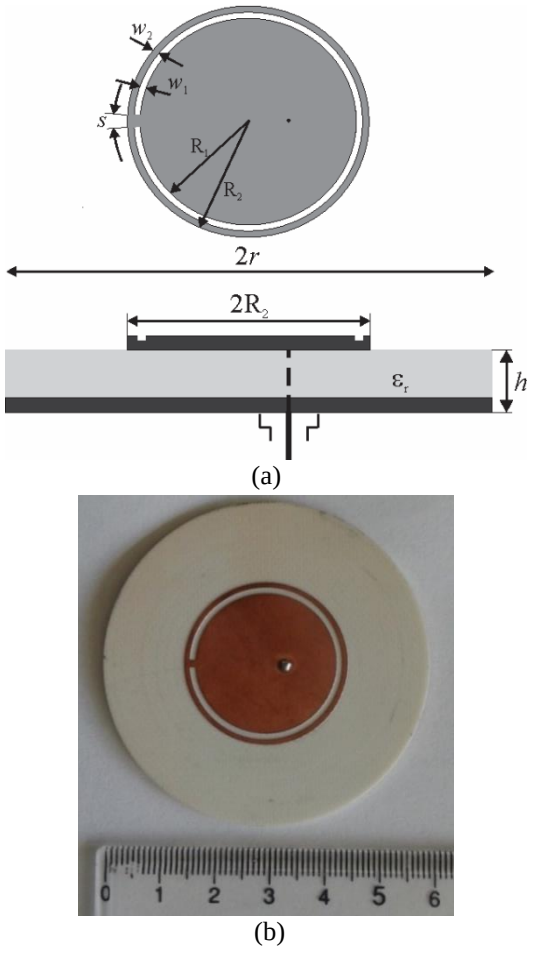

Fig. 3. Configuration of the circular patch antenna with a gap-ring-slot: (a) antenna geometry and layout, and (b) experimental model.

In order to design a low profile circular patch (CP) antenna that exhibits dual frequency operation, a narrow slot (w_1 = 1 mm) shaped like a ring with an annular gap (the gap angle s = 6˚) has been loaded into the radiated patch surface of radius R_2 = 15 mm close to the patch boundary. A distance of the slot from the patch edge is w_2 = 1 mm. In the given design, with R_1 and R_2 are marked radii of two circular patches, which contribute to the excitation of two resonant frequencies, both associated with the TM_{11} mode.

The optimal position of the coaxial feed providing an impedance matching between the feed and the antenna has been deduced according to the simulations for different feed positions with radius r_w = 0.15 mm (Fig. 4). According to the results, the optimum feed position for the fabricated antenna is set to be ρ = 3.5 mm, while relevant dimensions for the antena layout parameters have been chosen in accordance with the parametric study.

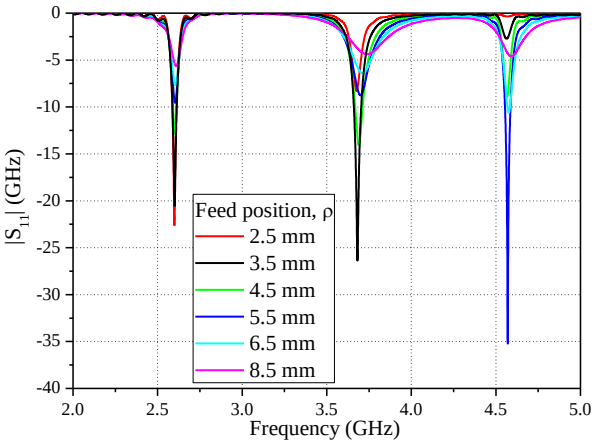

Fig. 4. Optimization of the feed position at the CP gap-ring-slot antenna.

IV. FREQUENCY ADJUSTMENT STUDY

Using the presented in-house solver based on an orthogonal polar TLM mesh, a parametric study has been carried out to explore the way in which finer design adjustments affect first two operating modes of the circular patch gap-ring-slot antenna. In this paper, we present a technique for independently tuning the lower resonant frequency of the antenna, followed by the technique for mutual adjustment of both resonant frequencies.

Figure 5 presents how a gap width s influences the resonant frequencies for the first two resonant modes (f_1 and f_2) and the frequency ratio. As shown, the angle of the gap affects more the lower resonant frequency than the higher one. By increasing the gap s, the lower mode is rising whereas the higher mode remains almost the same. In overall, by changing the gap spacing, the lower resonant frequency can be altered up to 8.4%, while the frequency ratio can be tuned in the range from 1.287 to 1.384. The corresponding dual frequency behaviour by listing the modes values with suitable bandwidth values (obtained from 10 dB return loss) is given in Table 1.

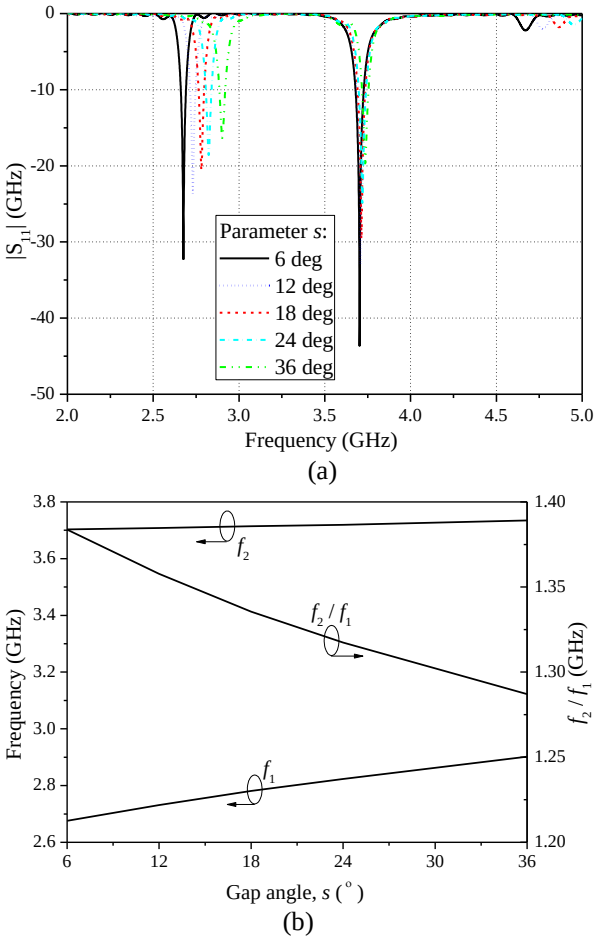

Fig. 5. Simulated results for the circular patch gap-ring-slot antenna with various gap angles s: (a) reflection coefficients, and (b) resonant frequencies and frequency ratio.

Table 1: Resonant frequencies and bandwidth of the CP gap-ring-slot antenna with various gap widths

Gap Spacing, s, (˚)	**f_1 (GHz)**	**BW (%)**	**f_2 (GHz)**	**BW (%)**	**f_2 / f_1**
6	2.676	1.15	3.703	1.29	1.384
12	2.731	1.15	3.708	1.27	1.357
18	2.781	1.17	3.714	1.21	1.335
24	2.823	1.17	3.719	1.17	1.317
36	2.902	1.16	3.735	0.99	1.287

Frequency adjustments of both operating modes of the circular patch gap-ring-slot antenna can be achieved by varying the ring-slot width w_1 or the width w_2. Influence of the widths w_1 and w_2 on resonant frequency

values is illustrated in Figs. 6. and 7, respectively. In contrast to the gap *s*, increasing the ring-slot width w_1 (while the radius R_2 remains constant), yields higher frequency to rise up to 8.5%, and the lower mode to decrease down to 3.7%. It is seen that the higher frequency is increased faster than the lower one is decreased. Also, the frequency ratio is tunable in the range from 1.325 to 1.494, as presented in Table 2.

On the other hand, the slot width w_2 (while the radius R_1 remains constant) affects more the lower mode which increase up to 6.3%, whereas the higher mode go down up to 1.65%, that is the frequency ratio is tunable in the range from 1.359 to 1.475, as presented in Table 3.

It can be concluded that the lower mode is more dependent on the radius R_2 of the circular patch, whereas the higher one mainly depends on the disk radius R_1. Therefore, due to different effects on the resonant modes, the dual-frequency operation with the tunable frequency ratio can be achieved.

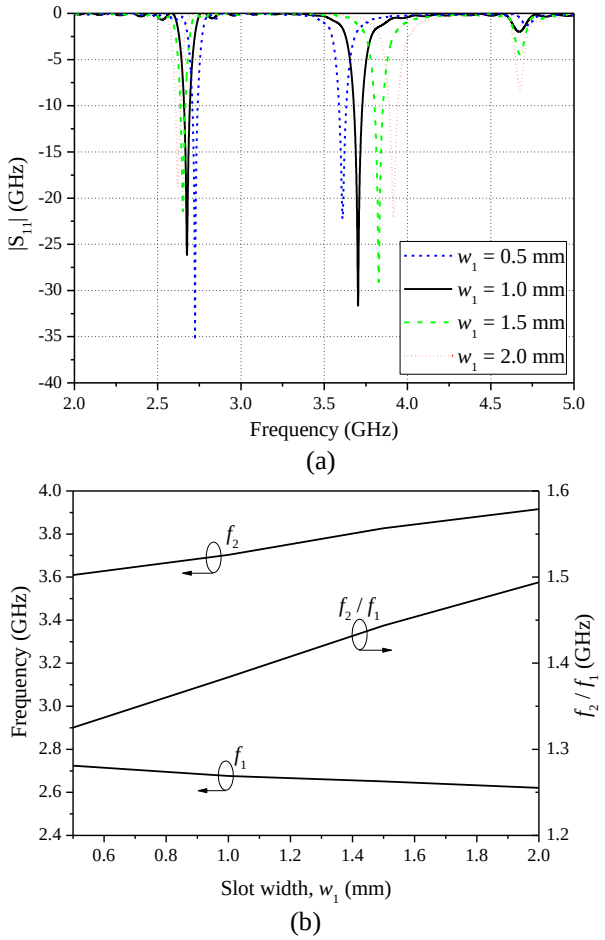

Fig. 6. Simulated results for the CP gap-ring-slot antenna with various ring slot widths w_1: (a) reflection coefficient, and (b) resonant frequencies and frequency ratio.

Table 2: Resonant frequencies and bandwidths of the CP gap-ring-slot antenna with various ring-slot widths, w_1

Ring-Slot Width, w_1, (mm)	f_1 (GHz)	BW (%)	f_2 (GHz)	BW (%)	f_2 / f_1
0.5	2.724	1.29	3.610	1.22	1.325
1.0	2.676	1.27	3.703	1.38	1.384
1.5	2.651	1.17	3.827	1.31	1.444
2.0	2.621	1.09	3.916	1.33	1.494

Table 3: Resonant frequencies and bandwidths of the CP gap-ring-slot antenna with various widths, w_2

Width, w_2, (mm)	f_1 (GHz)	BW (%)	f_2 (GHz)	BW (%)	f_2 / f_1
0.5	2.682	1.05	3.646	1.46	1.359
1.0	2.600	1.01	3.681	1.20	1.416
1.5	2.593	1.21	3.712	1.22	1.432
2.0	2.513	1.26	3.706	1.19	1.475

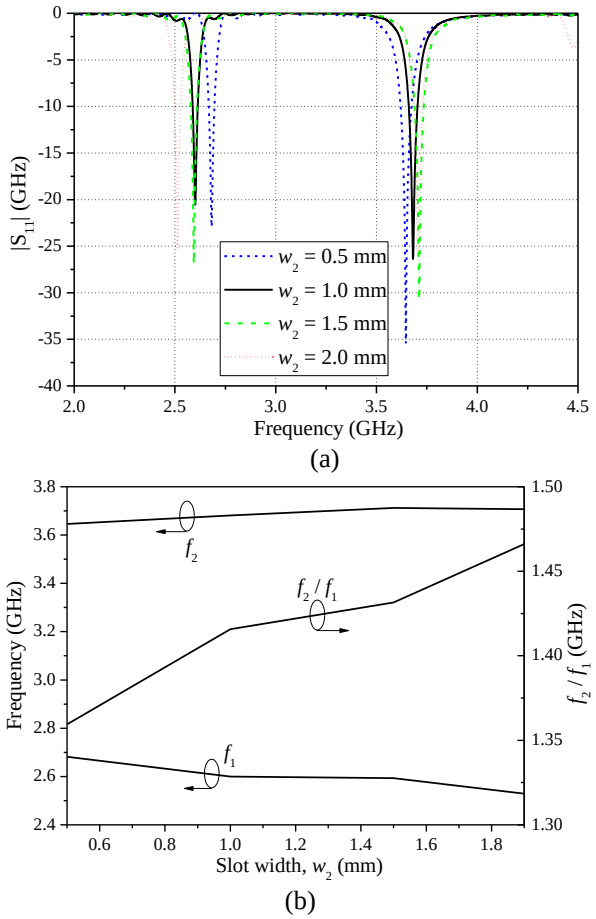

Fig. 7. Simulated results for various ring widths w_2: (a) reflection coefficient, and (b) resonant frequencies and frequency ratio.

Finally, Table 4 represents the comparison of antenna characteristics, such as frequency ratio and

bandwidth, between the fabricated proposed antenna and referenced antennas. By adjustment of the dimensional parameters of the proposed antenna, a small frequency ratio can be achieved which is an advantage in many applications.

Table 4: Comparison of frequency ratio and bandwidth

Ref.	1st BW (%)	2nd BW (%)	f_2 / f_1
[25]	1.4	1.8	2.0 ÷ 3.2
[26]	0.91 ÷ 1.17	1.04 ÷ 1.05	1.766 ÷ 1.983
[27]	6.9	0.6	1.28
[28]	0.48 ÷ 3.1	0.73 ÷ 6.1	1.58 ÷ 1.76
Here	1.05 ÷ 1.29	0.99 ÷ 1.46	1.287 ÷ 1.494

V. CYLINDRICAL MESHING CAPABILITIES

Mesh representations in the rectangular and cylindrical coordinate system for the CP gap-ring-slot antenna considered here are illustrated in Fig. 8. To ensure numerical results to be valid, it is requested to realize a TLM model which is in accordance with a physical antenna model as much as possible.

Since a radiated patch surface in the given design contains a narrow ring slot with a small angular gap, a specific attention during the modelling procedure has been put on these parameters. Opposed to a cylindrical mesh, where these features are described straightforwardly and accurately, a staircase approximation has had to be applied in a rectangular mesh. To explore benefits of the cylindrical meshing in contrast to the widespread rectangular mesh, different cell sizes have been used in both solvers and the most representative results are summarized in Fig. 9.

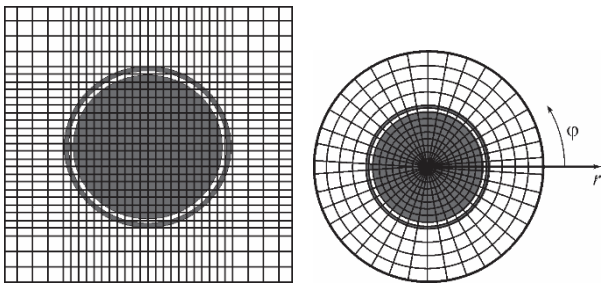

Fig. 8. Meshing in: (a) rectangular grid, (b) cylindrical grid.

As can be seen, the applied rectangular mesh ($\Delta x = \Delta y = \lambda/60$ within the substrate area, short-dash-dot line in Fig. 9.) does not provide expected results, i.e., only one resonant frequency is excited instead of two. This is definitely a consequence of not adequate meshing since the applied mesh does not allow for the relevant description of the narrow ring and the small angular gap (Fig. 8 (a)). Therefore, the rectangular mesh of higher resolution is inevitable to be used, such as for instance $\Delta x = \Delta y = \lambda/120$ within the substrate area, as shown in Fig. 9. (dash-dot line). Additionally, the cell size limits the radius of the wire feed used for excitation, which affects the resonant modes as well, and hence may lead to inaccuracies. Opposed to the rectangular mesh, the orthogonal polar mesh (Fig. 8 (b)) gives very good result even with the radial cell size $\Delta r = \lambda/60$ (short-dash-line in Fig. 9.), whereas the cell size $\Delta r = \lambda/120$ provides better results (dash-line in Fig. 9.). Note that cell size in the air-filled area along the specific axis is set up to be greater than within the substrate, due to maintaining time synchronism during simulations [3, 22].

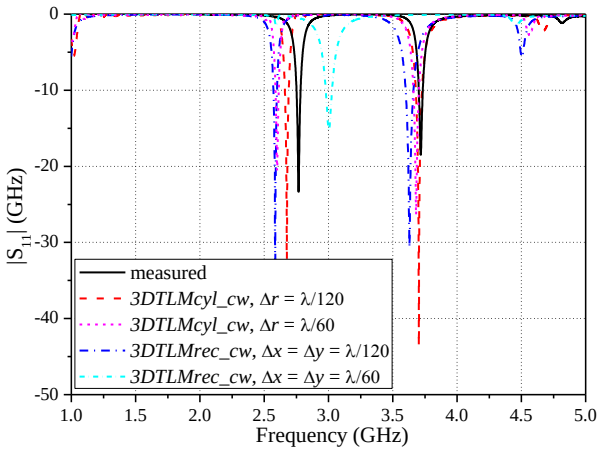

Fig. 9. Measured and simulated reflection coefficient for the circular patch antenna with a gap-ring-slot for different mesh resolutions.

In overall, limitations of the rectangular meshing heighten when applied to some specific structures that comprise narrow slots. From one hand, it is memory and time consuming due to the extremely higher number of cells used, and from the other hand, it cannot be resolved with a realistic wire radius, which instead has to be decreased so the simulation can proceed. On the other hand, advantages of the cylindrical meshing applied to the circular/cylindrical geometry are seen in accurate describing of fine annular and radial features accompanied with a less demanding computation since boundaries approximation is avoided as well as in the considerably reduced number of cells applied, leading to less memory for the storage, and more efficient scattering and connection procedures. If we assume that the number of nodes can be evaluated as Nx×Ny×Nz (Nx = Ny) in the rectangular mesh, and Nφ×Nr×Nz in the cylindrical mesh, and bearing in mind that Nr = Nx/2, while Nφ < Nx, it is easy to conclude that the cylindrical TLM demands much smaller number of cells than the rectangular TLM. To prove that, Table 5. summarizes cell dimensions and

a number of cells needed for modelling of the circular patch antennas with the gap-ring-slot in the cylindrical and rectangular TLM solvers.

Table 5: Properties of the cylindrical and rectangular TLM meshes applied to the CP gap-ring-slot antenna

Solver	Δx, Δy, Δr in Substrate (at 5GHz)	Mesh/ Number of Cells	Error (%)	
			1st Mode	2nd Mode
3DTLM rec_cw	λ/60	86×85×69/ 498.525	Invalid results	
	λ/120	184×185×69/ 2.348.760	6.5	2.4
3DTLM cyl_cw	λ/60	60×46×67/ 184.920	6.1	1.0
	λ/120	60×92×67/ 369.840	3.6	0.5

Obviously, the number of rectangular cells is considerably greater than the number of cylindrical cells making the cylindrical meshing much more efficient. According to the resonant frequency values errors relative to the experimental results, one can find that similar accuracy is achieved for λ/120 cell size in the rectangular mesh and λ/60 cell size in the cylindrical mesh, while the accuracy <5% for both simulated frequency values is achieved only for the cylindrical mesh with the cell size λ/120. Also, the rectangular mesh with λ/60 cell size cannot provide valid results due to inappropriate meshing. Note that a computational area in the cylindrical mesh for the case of λ/120 cell size is equal to 2π rad×60 mm×61.524 mm, whereas the computational area in the corresponding rectangular mesh is 120 mm×120 mm×61.524 mm.

VI. SIMULATED AND MEASURED RESULTS

The antenna characteristics have been measured on the network analyzer (VNA) and in an anechoic chamber of the Technische Universität Ilmenau, Germany.

Measured and simulated reflection coefficients for the proposed CP gap-ring-slot antenna are shown in Fig. 10. The plotted results correspond to the cell size $\Delta x = \Delta y = \lambda/120$ in the rectangular mesh and to the cell size along the r-axis in the cylindrical mesh that is equal to $\Delta r = \lambda/60$. The feed position in simulations has been adjusted accordingly. As can be seen from Fig. 10, two resonant frequencies (2.77 GHz and 3.72 GHz) instead of a single frequency for the conventional CP antenna are excited. Table 6 shows operating mode values obtained by measurements and simulations in both solvers. It can be found that the simulated results agree well with the measured result obtained by using the VNA. Discrepancies are the result of the fabrication procedure related to the slight deviation of slots dimension and feed positioning as well as the connectors and coaxial cable losses. A mutual agreement between simulated results obtained by rectangular and cylindrical mesh is satisfactory, but it has to be pointed out that considerably finer rectangular mesh has been applied compared to the cylindrical one, which was thoroughly investigated previously.

Table 6: Measured and simulated resonant frequency values for the CP gap-ring-slot antenna

Results	Resonant Frequency* (GHz)	
3DTLMcyl_cw	2.60	3.68
3DTLMrec_cw	2.59	3.63
Measured	2.77	3.72

*Results correspond to the cylindrical ($\Delta r = \lambda/60$) and rectangular ($\Delta x = \Delta y = \lambda/120$) TLM meshes.

The radiation pattern of the antenna is measured in the anechoic chamber, and it is illustrated in Fig. 11 (a) together with the simulated one. A good agreement is achieved. Results for two operating frequencies at 2.77 GHz and 3.72 GHz are shown in Figs. 11 (b) and 11 (c), respectively. It is seen that good broadside radiation patterns are obtained, with the maximum radiation in direction theta equal to 0 degrees. Also, similar broadside radiation characteristics can be observed for both of the operating modes, hence both resonant frequencies are associated with the TM_{11} mode. Results indicate that the peak antenna gain reaches about 6.2 dBi and 6.8 dBi, respectively for two operating modes. Therefore, the gain is slightly improved at higher resonant frequency.

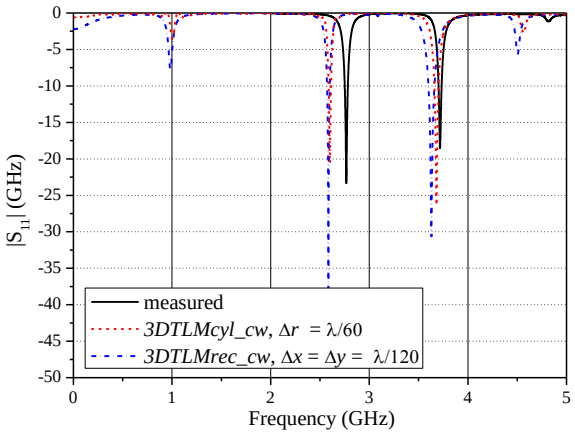

Fig. 10. Measured and simulated reflection coefficient for the circular patch antenna with a gap-ring-slot.

VII. CONCLUSION

In this paper, a dual-band coaxially fed circular patch antenna is designed by using the TLM method adapted to the orthogonal polar mesh and enhanced with the compact wire model. The antenna is realized on the Ro4003 substrate and contains a ring slot with an angular

gap, contributing to excitation of two resonant modes instead of one, thus making the antenna capable of dual frequency operation. A prototype of the designed antenna has been fabricated and measured. The measured results have been used to validate the cylindrical TLM approach. Advantages of applying the cylindrical mesh to the proposed antenna structure have been explored through comparison with the corresponding rectangular TLM mesh parameters. The cylindrical TLM has been proven as much more efficient than the rectangular TLM due to requested smaller number of applied cells, with capabilities of accurate describing of curvilinear boundaries including narrow ring slots and small angular gaps along with more possibilities related to modeling of realistic wire properties due to greater cell size.

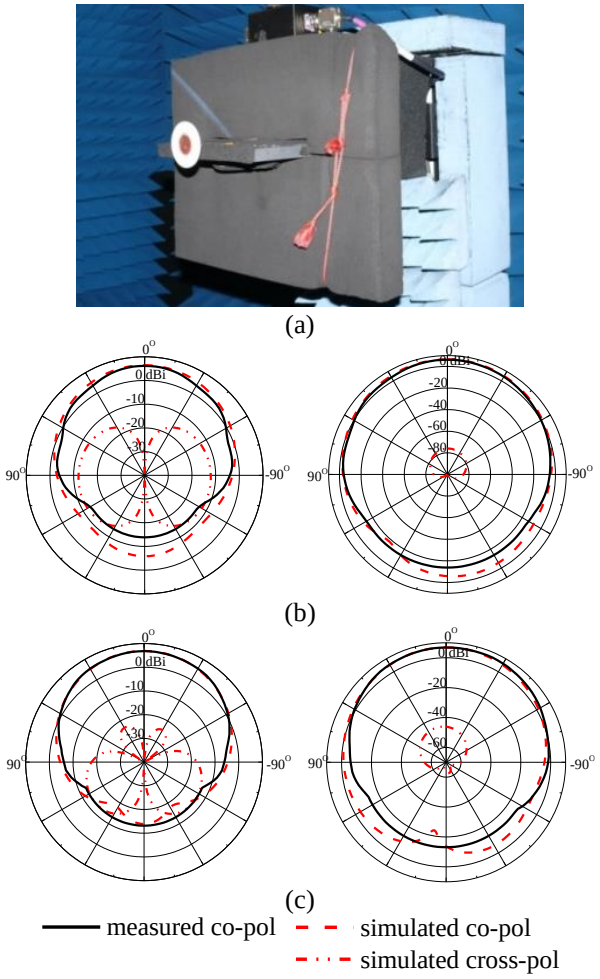

Fig. 11. Measurements in an anechoic chamber: (a) experimental setup, (b) measured and simulated E- and H-plane at 2.77 GHz, and (c) measured and simulated E- and H-plane at 3.72 GHz.

Results of a parametric study to explore frequencies adjustment capabilities of the presented antenna design have also been presented. A technique to achieve independent lower frequency adjustment has been introduced by varying the angular gap, while the mutual frequency tuning is shown to be possible by changing the ring-slot width. By adjusting the various geometric parameters, the frequency ratio and the bandwidth of each mode can be easily controlled.

Proven capabilities and efficiency of the cylindrical TLM approach will be of great help for the design of multi-band or reconfigurable circular patch antennas, containing very narrow angular or radial slots, which will be a part of the future investigation.

ACKNOWLEDGMENT

We want to thank the head of the RF and Microwave Research Laboratory of the Technische Universitaet Ilmenau Prof. M. A. Hein and Dr. Kurt Blau who helped us to realize the antenna samples and to carry out the measurements. This work was supported by the Ministry of Education, Science and Technological Development of Republic of Serbia (III44009 and TR32052).

REFERENCES

[1] C. A. Balanis, *Antenna Theory: Analysis and Design*. John Wiley & Sons, New York, 2012.

[2] R. Garg, *Microstrip Antenna Design Handbook*. Artech House, 2001.

[3] C. Christopoulos, *The Transmission-Line Modelling Method: TLM*. IEEE Press, 1995.

[4] https://www.cst.com, 2018.

[5] R. F. Harrington, *Field Computation by Moment Method*. *IEEE Press*, New York, 1993.

[6] A. Z. Elsherbeni and V. Demir, *The Finite-Difference Time-Domain Method for Electro-magnetics with MATLAB Simulations*. 2nd Edition (ACES Series on Computational Electromagnetics and Engineering). Edison, NJ: SciTech Publishing, an Imprint of the IET, 2015.

[7] J. R. Brauer, *Finite-Element Method*. Magnetic Actuators and Sensors, Wiley-IEEE Press, 2014.

[8] T. Z. Dimitrijevic, J. J. Jokovic, and N. S. Doncov, "Efficient modeling of a circular patch-ring antenna using the cylindrical TLM approach," *IEEE Antenn. Wirel. Pr.*, vol. 16, pp. 2070-2073, Apr. 2017.

[9] H. Tehrani and K. Chang, "Multifrequency operation of microstrip-fed slot-ring antennas on thin low-dielectric permittivity substrates," *IEEE Trans Antennas Propag.*, vol. 50, no. 9, pp. 1299-1308, Sep. 2002.

[10] X. L. Bao and M. J. Ammann, "Comparison of several novel annular-ring microstrip patch antennas for circular polarization," *J. Electromag. Waves Appl.*, vol. 20, no. 11, pp. 1427-1438, 2006.

[11] X. L. Bao and M. J. Ammann, "Microstrip-fed dual-frequency annular-slot antenna loaded by split-ring-slot," *IET Microwaves Antennas Propag*., vol. 3, no. 5, 757-764, July 2009.

[12] R. L. Farias, C. Lucatel, and M. V. T. Heckler, "Dual-band annular slot antenna for radio base stations," *The 8th European Conference on Antennas and Propagation (EuCAP 2014)*, The Hague, pp. 2055-2059, 2014.

[13] Y.-F. Lin, Y.-C. Kao, S.-C. Pan, and H.-M. Chen, "Bidirectional radiated circularly polarized annular-ring slot antenna for portable RFID reader," *ACES Journal*, vol. 23, no. 3, pp. 182-189, Mar. 2010.

[14] G. M. Kale, R. P. Labade, and R. S. Pawase, "Open rectangular ring slot loaded rectangular microstrip antenna for dual frequency operation," *Microw. Opt. Technol. Lett.*, vol. 57, pp. 2448-2452, July 2015.

[15] J. Kim, T. Jung, H. Ryu, J. Woo, C. Eun, and D. Lee, "Compact multiband microstrip antenna using inverted-L- and T-shaped parasitic elements," *IEEE Antennas Wirel. Propag. Lett.*, vol. 12, pp. 1299-1302, Sep. 2013.

[16] D. Guan, Z. Qian, W. Cao, L. Ji, and Y. Zhang, "Compact SIW annular ring slot antenna with multiband multimode characteristics," *IEEE Trans. Antennas Propag.*, vol. 63, no. 12, pp. 5918-5922, Dec. 2015.

[17] T. Dimitrijevic, J. Joković, and N. Doncov, "TLM modeling of an annular ring coupled to a circular patch with a shorting pin," *Proc. TELSIKS 2015*, Nis, Serbia, pp. 200-204, Oct. 2015.

[18] T. Dimitrijević, J. Joković, and N. Dončov, "Advantages of using integral cylindrical TLM method for modelling of coax-fed microstrip circular antenna," *Proc. TELSIKS 2013*, Nis, Serbia, pp. 200-204, Oct. 33-36, 2013.

[19] P. Sewell, T. M. Benson, C. Christopoulos, D. W. P. Thomas, A. Vukovic, and J. G. Wykes, "Transmission-line modeling (TLM) based upon unstructured tetrahedral meshes," *IEEE Trans. Microw. Theory Tech.*, vol. 53, no. 6, pp. 1919-1928, June 2005.

[20] X. Meng, P. Sewell, N. H. A. Rahman, A. Vukovic, and T. M. Benson, "Experimental benchmarking of unstructured transmission line modelling (UTLM) method in modelling twisted wires," *ACES Express Journal*, vol. 1, no. 3, pp. 101-104, Mar. 2016.

[21] H. Meliani, D. De Cogan, and P. B. Johns, "The use of orthogonal curvilinear meshes in TLM models," *Int. J. Numer. Model. Electron. Netw. Devices Fields*, vol. 1, no. 4, pp. 221-238, Dec. 1988.

[22] T. Dimitrijević, J. Joković, B. Milovanović, and N. Doncov, "TLM modeling of a probe-coupled cylindrical cavity based on compact wire model in the cylindrical mesh," *Int. J. RF Microw. Comput.-Aided Eng.*, vol. 22, no. 2, pp. 184-192, Mar. 2012.

[23] R. Scaramuzza and A. J. Lowery, "Hybrid symmetrical condensed node for the TLM method," *Electron Lett.*, vol. 26, no. 23, pp. 1947-1949, Nov. 1990.

[24] V. Trenkic, A. J. Wlodarczyk, and R. A. Scaramuzza, "Modeling of coupling between transient electromagnetic field and complex wire structures," *Int. J. Numer. Model. Electron. Netw. Devices Fields*, vol. 12, no. 4, pp. 257-273, July 1999.

[25] K.-L. Wong and W.-S. Chen, "Compact microstrip antenna with dual-frequency operation," *Electron. Lett.*, vol. 33, no. 8, p. 646, Apr. 1997.

[26] K.-P. Yang and K.-L. Wong, "Dual-band circularly-polarized square microstrip antenna," *IEEE Trans. Antennas Propag.*, vol. 49, no. 3, pp. 377-382, Mar. 2001.

[27] Nasimuddin, Z. N. Chen, and X. Qing, "Dual-band circularly polarized S-shaped slotted patch antenna with a small frequency-ratio," *IEEE Trans. Antennas Propag.*, vol. 58, no. 6, pp. 2112-2115, June 2010.

[28] D. Yu, S. Gong, Y. Wan, and W. Chen, "Omni-directional dual-band dual circularly polarized microstrip antenna using TM01 and TM02 modes," *IEEE Trans. Antennas Propag.*, vol. 13, pp. 1104-1107, June 2014.

Tijana Z. Dimitrijevic was born in Nis, Serbia, in 1977. She received the Dipl.-Ing., M.Sc. and Ph.D. degrees from the Faculty of Electronic Engineering, University of Nis, Serbia, in 2003, 2007, and 2015, respectively. From 2003 to 2008, she was a Researcher, and she is currently a Teaching Assistant with the Department of Telecommunications, University of Nis, Serbia. Her main research interests include computational developments and application of the numerical TLM method for the purpose of an investigation of microwave applicators and microstrip antennas. She was the 2006 recipient of the Nikola Tesla National Award in Creativity of the Young category.

Jugoslav J. Jokovic was born in Novi Pazar, Serbia, in 1974. He received the Dipl.-Ing., M.Sc., and Ph.D. degrees from the Faculty of Electronic Engineering, University of Nis, Serbia, in 2000, 2004 and 2007, respectively. In 2000, he joined the Department of Telecommunications, University of Nis, Serbia, where he is now a Research and Teaching Assistant. His current research

interests include theoretical developments and experimental verification of the numerical TLM method and its application to EMC and microwave heating.

Nebojsa S. Doncov was born in Nis, Serbia, in 1970. He received the Dipl.-Ing., M.Sc., and Ph.D. degrees from the Faculty of Electronic Engineering, University of Nis, Serbia, in 1995, 1999 and 2002, respectively. From 1995 to 2001, he was with the Department of Telecommunications, Faculty of Electronic Engineering, Serbia, as a Research Assistant. From 2001 to 2004 he was working with Flomerics Ltd, Electromagnetics Division, U.K., as a Research and Development Engineer. In 2004, he joined the Department of Telecommunications, Faculty of Electronic Engineering, Serbia, where he is now a Full Professor. His current research interests are in computational and applied electromagnetics with a particular emphasis on TLM and network methods applications in microwaves and EMC. Doncov was the recipient of the International Union of Radio Science (URSI) Young Scientist Award in 2002.